BIOGEOCHEMICAL EVOLUTION OF THE WESTERN INTERIOR BASIN OF NORTH AMERICA DURING A KASIMOVIAN HIGHSTAND AND REGRESSION

A Thesis

by

SIKHAR BANERJEE

Submitted to the Office of Graduate Studies of
Texas A&M University
in partial fulfillment of the requirements for the degree of

MASTER OF SCIENCE

December 2011

Major Subject: Geology

Biogeochemical Evolution of the Western Interior Basin of North America

during a Kasimovian Highstand and Regression

BIOGEOCHEMICAL EVOLUTION OF THE WESTERN INTERIOR BASIN OF NORTH AMERICA DURING A KASIMOVIAN HIGHSTAND AND REGRESSION

A Thesis

by

SIKHAR BANERJEE

Submitted to the Office of Graduate Studies of
Texas A&M University
in partial fulfillment of the requirements for the degree of

MASTER OF SCIENCE

Approved by:

Co-Chairs of Committee,	Anne Raymond
	Mike Tice
Committee Members,	Ethan Grossman
	Vaughn Bryant
Head of Department,	Rick Giardino

December 2011

Major Subject: Geology

ABSTRACT

Biogeochemical Evolution of the Western Interior Basin of North America during a Kasimovian Highstand and Regression. (December 2011)

Sikhar Banerjee, B.S., Pune University, Pune;

M.S., Indian Institute of Technology-Bombay

Co-Chairs of Advisory Committee: Dr. Anne Raymond
Dr. Mike Tice

The purpose of this study is to identify and analyze the geochemical facies of the Hushpuckney Shale using XRF scanning data and the bioturbation indices, which will contribute to a better understanding of the biogeochemical environment prevalent during the deposition of the Hushpuckney Shale.

The Hushpuckney Shale Member of the Swope Formation (Kasimovian Stage) preserved in KGS Spencer core 2 – 6, consists of a black shale submember overlain by bioturbated gray shale. Millimeter-scale core description and analysis of XRF scanning data enables identification of geochemical facies within the study core and contributes to understanding the environment of shale deposition. The XRF spectrometer produces X-ray image of the core and abundance values of selected major and trace elements, including iron (Fe), calcium (Ca), sulfur (S), molybdenum (Mo), zinc (Zn), vanadium (V), chromium (Cr), copper (Cu), nickel (Ni), titanium (Ti), zircon (Zr), potassium (K) and phosphorous (P). Canfield and Thamdrup's (2009) classification of geochemical environments is used to recognize oxic/aerobic, manganous-nitrogenous, ferruginous

and sulfidic facies within the black shale submember. A modification of Droser and Bottjer's (1986) semi-quantitative field classification of bioturbation is used to identify facies variations within the gray shale submember. Abundance of apatite nodules and lamina in the black shale submember of the study core suggest that black shale sediments accumulated slowly in a sediment-starved basin. A high abundance of sulfide-scavenged elements, including Mo, Zn, V, Ni and Cr, identifies the sulfidic facies in the black shale submember, and indicates deposition in an oxygen-depleted environment with a high concentration of hydrogen sulfide. The overlying ferruginous facies has lower abundances of sulfide-scavenged elements and lacks cryptic Fe-laminations. The uppermost black shale submember facies, the manganous-nitrogenous facies, has cryptic Fe laminations and a relatively high P/Ca ratio. Abundance of cryptic iron laminations and apatite nodules and lamina indicates the syngenetic deposition of iron and phosphate due to Fe-P coupling mechanism. The gray shale submember is burrowed, indicating deposition under oxygenated conditions. Bioturbation indices reveal the variations in the intensity and nature of burrows within the gray shale, which corresponds to the changes in the depositional environment that may be related to the rise and fall of sea-level.

DEDICATION

To my family and all the teachers who have inspired me throughout my academic life.

ACKNOWLEDGEMENTS

I would like to thank my committee chair, Dr. Anne Raymond, my committee co-chair, Dr. Mike Tice and my committee members, Dr. Grossman and Dr. Bryant for their guidance and support throughout the course of this research.

Thanks also to my friends and colleagues and the department faculty and staff for making my time at Texas A&M University a great experience. I also want to extend my gratitude to the Hess Corporation and ConocoPhillips for their financial support, to Kansas Geological Society for providing the shale core, which was essential for this study and to all the professors and students who were willing to participate in the study.

Finally, thanks to my mother and father for their encouragement and love.

NOMENCLATURE

B.I.	Bioturbation Index
Ca	Calcium
Cr	Chromium
Cu	Copper
Fe	Iron
FFT	Fast Fourier Transform
K	Potassium
MFS	Maximum Flooding Surface
Mn	Manganese
Mo	Molybdenum
Ni	Nickel
P	Phosphorous
S	Sulfur
Ti	Titanium
U	Uranium
V	Vanadium
XRF	X-Ray Fluorescence
Zn	Zinc
Zr	Zirconium

TABLE OF CONTENTS

Page

ABSTRACT iii

DEDICATION v

ACKNOWLEDGEMENTS vi

NOMENCLATURE vii

TABLE OF CONTENTS viii

LIST OF TABLES x

LIST OF FIGURES xi

1. INTRODUCTION 1

2. MATERIALS 7

3. METHODS 8

    3.1 Core description 8
    3.2 XRF scanning 8
    3.3 Geochemical facies classification 10
    3.4 Bioturbation index classification 12

4. RESULTS 13

    4.1 Core description 13
    4.2 X-Ray fluorescence mapping 14
    4.3 Bioturbation 16

5. DISCUSSION 17

6. CONCLUSION 24

REFERENCES 26

APPENDIX 33

Page

VITA…….. 43

LIST OF TABLES

TABLE Page

1 Average gray values of elements in ferruginous and sulfidic facies..... 33

LIST OF FIGURES

FIGURE Page

1 Cyclostratigraphy of Kansas-type cyclothemic core shales and inferred distribution of time…….....34

2 Paleogeography of Late Pennsylvanian North America ..... …35

3 Generalized stratigraphic column of Kansas City Group in the outcrop ... …36

4 Depth distribution of common electron acceptors and the corresponding geochemical facies..... 37

5 Iron laminations within the study core unit identified using the FFT technique …….....38

6 Bioturbation indices for the different geochemical facies of the Hushpuckney Shale. ..... …39

7 Laminations shown by apatite (Ca_3PO_4) within the study core……...40

8 Relative abundance of various sulfide-scavenged elements (Mo, Zn, V, Ni, Cr) in the study core…….. 41

9 Relative abundance of various major elements (Fe, S, Ca, P) in the study core…… ……42

1. INTRODUCTION

Organic-rich marine shales are important hydrocarbon source rocks (Arthur and Sageman, 1994). Pennsylvanian organic-rich shales accumulated in response to glacial-eustatic fluctuations in sea-level driven by the advance and retreat of continental ice sheets on Milankovitch time scales (Cruse and Lyons, 2004; Schultz, 2004). During the Pennsylvanian, as sea level fluctuated, coastal peat swamps and lagoons were inundated, and organic-rich, metalliferous black shales were deposited. The Hushpuckney Shale (Swope Formation) is an organic-rich shale deposited during the late transgressive to early regressive phases of the Late Pennsylvanian (Kasimovian Stage) glacio-eustatic Swope cycle (Heckel, 1994: Figure 1). The Hushpuckney Shale and the underlying limestone, which accumulated in the western Interior Basin of North America, may be contemporaneous with the Brush Creek Coal and the overlying marine facies in northern Appalachian basin (Kosanke and Cecil, 1996; Peppers, 1996: Figure 2). Thus, the Hushpuckney shale may record terrestrial climatic and environmental changes that are difficult to trace in terrestrial and shallow marine sediments due to erosion and non-deposition. Hence, it was of utmost importance to find a comprehensive method which can be used to recognize the biogeochemical variations within the shale core in order to better understand the changes in the depositional environment during the deposition of the Hushpuckney Shale.

This thesis follows the style of *Paleogeography, Paleoclimatology, Paleoecology*.

The Hushpuckney Shale member (Figure 3) consists of a black shale submember, overlain by a gray shale submember, interpreted as a change from anoxic to progressively dysaerobic conditions (Algeo et al., 2004; Schultz, 2004.). The Hushpuckney Shale was divided into four redox zones including increasing euxinia, decreasing euxinia, fluctuating anoxia and dysoxia, based on the stratigraphic trends of the "redox-indicator trace" elements including Mo, U, V and Zn (Algeo and Maynard, 2004). Algeo et al. (2004) observed that the black shale submember shows a shift from organic macerals of mixed terrestrial-marine origin to a predominantly marine origin at about 30 cm, which is consistent with the increased abundance of authigenic phosphatic granules observed at the horizon (28-34 cm) and a change in the redox facies from uniformly euxinic to fluctuating anoxic conditions (30-35 cm). Based on the trends of "redox-indicator" elements, the entire gray shale submember were assigned to the dysoxic redox zone hence is insufficient in recognizing the geochemical variations within the gray shale submember. However using X-radiography, Algeo and Maynard (1997) were able to successfully correlate the core sections of the Hushpuckney Shale from different locations, at a centimeter scale. Thus, X-radiography can identify the redox zones present within the Hushpuckney Shale cores and these redox zones can be correlated throughout the basin.

Conventional schemes of environmental classification often refer to the zone that contains oxygen and supports metabolic aerobic metabolisms as the 'oxic' zone (> ~ 2.0 ml O_2 l^{-1} H_2O), and to oxygen depleted zones as 'suboxic' (~ 2.0 - 0.2 ml O_2 l^{-1} H_2O), 'anoxic' (< ~ 0.2 ml O_2 l^{-1} H_2O), 'euxinic' (0 ml O_2 l^{-1} H_2O, with free H_2S) zones

(Wignall, 1994). Anoxic zones support sulfate reduction and methanogenesis, whereas nitrate reduction, manganese reduction and iron reduction are believed to occur in the suboxic zone. Canfield and Thamdrup (2009) observed that this scheme is inherently ambiguous. In some marginal continental environments, bottom waters are anoxic while surface waters are oxic. Canfield and Thamdrup (2009) observed that sediments deposited in such environments are often classified as 'sub-oxic'. For example in the Black Sea and the Cariaco Basin, 'suboxic' processes such as Mn, Fe, and nitrate reduction take place in 'anoxic' water (Kuypers et al., 2003; Percy et al., 2008). The term 'suboxic sediments' is even more confusing because coastal sediments deposited under normal oxygenated waters can have sulfidic pore waters (Canfield and Thamdrup, 2009).

Canfield and Thamdrup (2009) proposed using the preference of the electron acceptor as a basis to classify the geochemical facies within sediments (Figure 4). The sulfidic facies, conventionally assigned to the anoxic zone, is characterized by sulfate reduction and the accumulation of dissolved sulfide. In sediments with abundant iron, the presence of iron sulfides identifies this facies (Canfield et. al., 1992; Canfield and Thamdrup, 2009). The ferruginous facies, conventionally assigned to the suboxic zone, is characterized by iron reduction and the accumulation of dissolved Fe^{2+}. This facies has seldom been described from sediments (Canfield and Thamdrup, 2009). The nitrogenous facies, conventionally assigned to the suboxic zone, is characterized by anaerobic ammonium oxidation, nitrite accumulation and nitrate reduction. This facies is difficult to identify in sediments (Canfield and Thamdrup, 2009). The manganous

facies, conventionally assigned to the suboxic zone, is characterized by the accumulation of dissolved Mn^{2+}. This facies may overlap in both its upper and lower bounds with other geochemical facies and is difficult to identify in argillaceous sediments (Canfield and Thamdrup, 2009). Canfield and Thamdrup (2009) identify the facies containing oxygen, in which aerobic respiration occurs, as oxic or aerobic. Analyzing of the geochemical profiles of the major and minor elements in the sediments can indicate the biogeochemical environments prevailing at the time of deposition.

Droser and Bottjer (1986) proposed a bioturbation index to facilitate field classification of ichnofabrics based on pattern recognition of the percentage of original sedimentary fabric in lower Paleozoic carbonates in the Great Basin region of California, Nevada and Utah. Furthermore, O'Brien (1987) used X-radiography to reveal the variations in the macro- and microfabrics found in shales. Algeo and others (2004) used this index to identify subtle bioturbation features in the X-radiograph of a Hushpuckney Shale core, and to infer patterns of benthic oxygenation.

In the study of sediment cores, a major technical advancement has been in form of the use of micro-X-ray fluorescence (XRF) and micro-X-radiograph scanner designed for rapid, automatic, non-destructive characterization of the optical, density and chemical compositional variations in split sediment cores (Croudace et. al., 2006). XRF spectrometer can scan cut core sections in order to obtain high-resolution geochemical profiles for that sediment core section. The geochemical data obtained from the XRF core scanners were mainly applied in the study of climate-driven cyclicity observed in

the sediment deposition, which for instance, can be used as evidences in understanding the evolution of global glacial-interglacial cycles of the Pleistocene (Jahn et. al., 2003). Moreover, continuous XRF profiling contributed to the lithostratigraphic analysis of deep-sea basin cores to identify features such as ash layers, turbidite units and ice-rafted deposits which may facilitate the provenance analysis of the basin core sediments (Hebbeln and Cortes, 2001; Richter et. al., 2001). Rothwell et al., (2006) used XRF scanning in a high-resolution geochemical and sedimentological study of the upper part of a piston core from the SE Balearic Abyssal Plain in the western Mediterranean Sea. These workers used XRF scanning images to obtain valuable information on textural grading, bioturbative mixing and found that Ca/Fe ratios were an effective parameter in distinguishing between turbidites and pelagites. Furthermore, XRF core scanner data can identify the marker beds, which are obscure when visually logged but geochemically distinct within the downcore elemental profiles, thereby facilitating the complete subdivision of a sequence into genetically related lithological units (Rothwell et. al., 2006).

This study applies XRF scanning data to identify the Canfield and Thamdrup geochemical facies within the black shale submember of the Hushpuckney Shale. However, the efficiency of the Canfield and Thamdrup scheme of classification was found to be inadequate to identify the different facies present in the gray shale submember as gray shale was deposited under oxygenated environment. Detailed fabric analysis including analyzing the presence of remnant laminations and the intensity of bioturbation, can determine the sedimentological factors influencing biogenic activity

(O'Brien, 1987). Droser et al., (1986) observed that bioturbation indices for each facies can be designated in the field by measuring the percentage of disrupted sedimentary fabric and the nature of the burrows present. Adapting this scheme of classifying ichnofabric to the X-ray images of the sediment core sections of the Hushpuckney Shale, bioturbation indices for the facies present in both the black and the gray shale submember can be obtained which would indicate the intensity of bioturbation. The degree of bioturbation, determined from detailed core description and X-radiography of the core, is effective in recognizing the facies present within the gray shale submember. Thus, the bioturbation indices combined with geochemical profiles of selected elements derived from the XRF scanning data, can identify the various geochemical facies variations within the Hushpuckney Shale. The purpose of this study is to analyze the geochemical facies of the Hushpuckney Shale which will contribute to a better understanding of the biogeochemical environment prevalent during the deposition of the Hushpuckney Shale.

2. MATERIALS

The Hushpuckney Shale was studied in the Kansas Geological Survey (KGS) Spencer 2 - 6 core, recovered by Colt Energy from Franklin County, Kansas (Sec 6, Twp. 18S, Range 21E; 38.51^{o} N, 95.13^{o} W). In this core, the Hushpuckney Shale consists of laminated black shale overlain by bioturbated gray shale. The entire unit is 134 cm thick and ranges from a depth of 11245.55 cm to 11379.55 cm.

3. METHODS

3.1 *Core description*

Detailed sedimentological study has the potential to reveal valuable textural clues to the depositional history of shales (Schieber, 2003). The sedimentary features that are hidden within the black shales divulge critical information about the environment of deposition, which can be used to infer the sedimentary and geochemical processes. I described the Hushpuckney Shale core at the centimeter scale depicting the distribution of apatite bands and nodules, bioturbation and sediment color.

3.2 *XRF scanning*

The X-ray fluorescence (XRF) spectrometer is an X-ray instrument used for bulk chemical analysis of major and trace elements in rocks. The major and trace elements of the rocks are excited when high-energy, short wavelength radiation (X-ray beam) illuminates them. The atoms in the sample absorb X-ray energy by ejecting electrons from the inner, lower energy levels and replacing them with electrons from an outer, higher energy orbital. This process is associated with the release of energy because the binding energy of inner electron orbitals is less than that of an outer one. This energy is emitted in the form of fluorescent X-rays, characteristic of a transition between specific electron orbitals in a particular element thereby detecting the abundances of the elements that are present in the sample (Fitton, 1997; Jansen et. al., 1998). I conducted XRF scanning of the entire Hushpuckney Shale core using a Horiba Jobin Yvon XGT-7000

energy-dispersive XRF spectrometer with a rhodium target at Texas A&M University to acquire fluorescence intensity values (number of counts per second) which for a constant matrix is proportional to the abundance values of various major and sulfide-scavenged elements in a stratigraphic context. Along with data on the stratigraphic abundance of elements I have also obtained X-ray images of the core. These analyses were conducted using a 50 kV accelerating voltage, a 1 mA current, 100 μm spot size with average dwell time per spot as 0.06 s and dead time of <20%. Integrated intensity of K lines for the following elements: Fe, S, Ca, P, Ti, Zr, K, Mo, Zn, V, Ni and Cr were calculated from full spectra at each point and corrected for background intensity. Moreover, I processed XRF scans and X-rays using 'ImageJ' software to increase clarity and contrast. I generated false color images using the RGB (Red-Green-Blue) color scheme, in which individual colors indicate individual elements. Using ImageJ, I derived tabular data of the bulk abundance of individual elements with stratigraphic depth. I prepared depth versus abundance graphs for selected elements in Microsoft Excel. Subsequently, I performed lowess regression analysis of the abundance values of each element using 'R' statistical software. I constructed the lowess values against depth in order to indicate local trends within the study core.

The ImageJ software package has a special module called Fast Fourier Transform (FFT), which can transform an image from spatial or intensity space into frequency space. The FFT module will filter a particular image, which depicts the abundance of a particular element into the fundamental intensity frequencies (Ayres et al., 2008). FFT analysis can reveal the repetitive occurrence of a particular element in a preferred orientation,

indicating the presence of microscopic laminae, which might otherwise be difficult to identify. I have used this technique to identify laminations of selected elements in the Hushpuckney shale. The regions from the core which is assumed to have cryptic laminations of iron are selected for the FFT analysis. Furthermore, within the selected region, the areas that do not have apatite laminations are chosen in order to avoid interference effects of calcium. When subjected to FFT processing, these areas exhibit the presence of cryptic iron laminations in a favored orientation (Figure 5).

3.3 *Geochemical facies classification*

In this study, I identified four geochemical facies in the Hushpuckney Shale based on trace fossils and XRF scanning data. The 'aerobic' facies can be identified by the presence of burrows attributed to the benthic organisms, which require oxygen (Drosser and Bottjer, 1988).

In sediments, the nitrogenous facies can be identified by nitrite accumulation (Morrison et. al., 1999; Codispoti et. al., 2001); and the manganous facies by accumulation of Mn. Moreever, the manganous facies can overlap in both the upper and lower bounds with other geochemical facies (Postma and Appelo, 2000; Schippers et. al., 2005). Because of this overlap, separating the manganous facies from the nitrogenous facies is not feasible (Canfield and Thamdrup, 2009). Accordingly, in this study, these two facies have been combined into a 'manganous-nitrogenous' facies.

In sediments, the manganous-nitrogenous sedimentary facies belongs to the conventional 'suboxic' facies, which is defined by the absence of bioturbation and

presence of ferric iron (Fe^{3+}) as ferric oxhydroxides (Canfield et. al., 1993), which in low oxygenated environments will form iron laminae. In the Hushpuckney Shale, the absence of bioturbation and the presence of cryptic iron laminations can be used to distinguish manganous-nitrogenous facies from other facies.

The ferruginous facies is characterized by the presence of ferrous iron (Fe^{2+}) in solution. Because iron is in this facies is in the soluble reduced oxidation state, there are no cryptic ferric oxide laminations. In the sediments within the ferruginous facies, even a small amount of sulfide in the water column leads to the deposition of sulfide-scavenged elements, including Mo, Zn, V and Ni. Enrichment of Zn, V, and Ni in sediments occurs predominantly due to the formation of sulfides; whereas Mo is transformed into thiomolybdate compounds allowing subsequent removal from solution via metal sulfides or organic matter (März et al., 2008). In the Hushpuckney Shale, the absence of cryptic ferric oxide laminations and intermediate levels of sulfide-scavenged elements, including Mo, Zn, V and Ni, identifies the ferruginous facies.

The sulfidic facies is characterized by high abundances of sulfide-scavenged elements (Mo, Zn, V, Cr and Ni). Sulfide-scavenged trace elements including Mo, Zn, V, Cr and Ni can be used as fairly reliable recorders of oxygen-deficient to sulfidic depositional conditions (März et. al., 2008). Conventionally, the sulfidic facies is referred to as euxinic. If there is sufficient reactive iron in solution, then ferrous sulfides or pyrites will form (Canfield and Thamdrup, 2009). Thus, the presence of pyrite would identify sulfidic facies though this is not a necessary condition.

3.4 *Bioturbation Index classification*

Droser and Bottjer (1986) proposed a semi-quantitative field classification of bioturbation. I have adapted this classification to quantify bioturbation evident in the X-ray images of the Hushpuckney shale core in terms of index numbers (Figure 6). Index number 1 indicates that lamination is continuous and is well preserved while Bioturbation index 2 suggests that the laminae are discontinuous with evidences of the presence of burrows. Bioturbation index in the range of 3 is characterized by 10% ~ 40% of disrupted lamination and numerous burrows which are isolated and locally overlap. Bioturbation index number 4 indicates that nearly 40% ~ 60% of laminations are disrupted with overlapping burrows mostly indistinct. Index number 5 is suggests that the facies is dominantly (~90%) homogenized but some discrete burrows may be present. Ichnofabric index number 6 represents completely homogenized sediment. Bioturbation disrupts primary sedimentary fabric so it is possible to measure the degree of disruption using X-ray fluorescence images of the study core unit. In this study, the classification scheme proposed by Droser and Bottjer (1986) is used to quantify the bioturbation (Figure 6). This scheme is originally based on the semi-quantitative field classification of ichnofabric but for the present study, it has been modified to be applicable to the X-ray images.

4. RESULTS

4.1 *Core description*

The entire study core of the Hushpuckney shale, which is about 134 cm thick, consists of a black shale submember (~72 cm) grading into a gray shale submember (~58 cm). The Middle Creek Limestone Formation lies beneath the Hushpuckney shale. This limestone formation is a phylloid algal wackestone which near the contact with the black shale submember has microstylolites. The stratigraphic contact of the Hushpuckney shale with the underlying Middle Creek Limestone formation is sharp in nature and irregular in relief. The black shale submember is weakly bioturbated near this contact. The black shale submember is laminated and exhibits abundance of apatite nodules and laminae however it lacks fossil fragments. Laminations in the black shale are predominantly 2 - 3 millimeters thick and characterized by elliptical apatite nodules and organic matter. Macroscopic apatite nodules are prevalent throughout the entire black shale submember but are absent at certain intervals (~ 18 - 22 cm and ~ 34 - 41 cm.

In contrast to the black shale, the overlying gray shale submember has abundant trace fossils. Moreover, within the gray shale submember the color of the matrix changes from darker to lighter shades of gray in a cyclic pattern. Within the contact region between the black and the gray shale submember which is gradational in nature, *Trichichnus* burrows (0.4 - 1 cm in horizontal diameter) can be observed. The burrows are elliptical in cross-section and are both vertical and lateral in nature. In the vicinity of

the upper contact between the Hushpuckney shale and the fossiliferous wackestone of the Bethany Falls Limestone member, the gray shale submember is fossiliferous.

4.2 *X-Ray fluorescence mapping*

Following the Canfield and Thamdrup (2009) classification for geochemical environments, the study core reveals the presence of the following geochemical facies namely sulfidic, ferruginous, manganous-nitrogenous and aerobic facies. The basal part of the black shale submember, which lies above the Middle Creek Limestone, is classified as aerobic facies (~ 11384.30 - 11369.60 cm) because this region is bioturbated. Above the basal aerobic facies lies a manganous-nitrogenous facies (~ 11369.60 - 11363.75 cm), which is characterized by the presence of cryptic Fe-lamination and the absence of bioturbation. At the top of this manganous-nitrogenous facies, there is a particular region (~11366.60 - 11363.75 cm) which exhibits presence of strong bands of apatite combined with abundance peak of Ti and K. The next interval, which is defined by the absence of iron laminations and intermediate abundance values of sulfide-scavenged trace elements, is the ferruginous facies (~ 11363.75 - 11362 cm). Abundances of sulfide-scavenged elements in the ferruginous facies are higher than in manganous-nitrogenous facies, but conspicuously lower than in the sulfidic facies (Table 1). The region just above the ferruginous facies (~ 11356 - 11360 cm) has the highest abundances of sulfide-scavenged elements including Mo, Zn, V, Ni, Cr, Cu and S, within the entire Hushpuckney shale core. The highest abundance values of V and Ni occur within a relatively broader zone (~ 11338 - 11358 cm) within the study core

whereas higher abundances for Cr occur in a broad zone (~ 11327 - 11351 cm) within the study core. Sulfidic conditions prevailed during the deposition of a substantial portion of the black shale submember (~ 11362 - 11328.50 cm). In the stratigraphic succession, above the sulfidic facies there is another core interval assigned to the ferruginous facies (~ 11328.50 - 11327 cm) followed by another interval consigned to the manganous-nitrogenous facies (~ 11327 - 11300 cm).

The entire gray shale submember shows distinct evidence of bioturbation and is assigned to the aerobic facies. Moreover, based on the density and orientation of burrows, the aerobic facies within the gray shale submember is further divided into aerobic burrowed and aerobic homogenized facies. Three 'Aerobic Burrowed' intervals consist of argillaceous (Fe-rich) mud and have an abundance of burrows (mostly horizontal and a few vertical) (~ 11297 - 11282.55, 11269 - 11261.40, 11251.65 - 11246.40 cm). The 'Aerobic Homogenized' facies consist of calcareous mud and is mostly homogenous with very few vertical burrows (~ 11282.55 - 11269, 11259.70 - 11251.65 cm). The gray shale submember grades into the overlying Bethany Falls limestone member that is characterized by increases in calcium content and the abundance of fossils such as brachiopods.

Visible laminations in the black shale submember are predominantly composed of apatite. Layers of apatite granules and nodules occur throughout the ferruginous, manganous-nitrogenous and sulfidic facies (Figure 7). However, apatite lamination is most prominent within the sulfidic facies. Cryptic laminations of ferric iron also occur in

the core and were used to define the manganous-nitrogenous facies. Although these cryptic laminations are not visible under the microscope, they can successfully be detected using FFT processing.

4.3 *Bioturbation*

The aerobic burrowed facies at the base of the black shale submember has been assigned Bioturbation index 2. This layer is weakly burrowed and has discontinuous (apatite) laminae. The sulfidic facies and all of the ferruginous and manganous-nitrogenous facies found within the black shale submember have been assigned the number 1 in the bioturbation index scale as they exhibit distinct laminations that are continuous across the width of the core. The overlying gray shale submember has been further divided into aerobic burrowed and aerobic homogenized facies based on the degree of bioturbation. Each facies present within the gray shale submember exhibiting varying intensity of bioturbation has several bioturbation indices. Therefore, the gray shale submember has been assigned a host of the bioturbation index numbers: 3 (~ 11294.30 - 11290.30 cm), 4 (~ 11296.90 – 11294.30, 11290.30 – 11283.60, 11264.60 – 11262.30, 11251.75 – 11245.30 cm), 5 (~11283.60 – 11278.20, 11269 – 11264.60, 11258.60 – 11251.75, 11245.30 – 11242.15 cm) and 6 (~ 11278.20 - 11269, 11262.30 – 11258.60 cm).

5. DISCUSSION

The Canfield-Thamdrup classification of geochemical facies enables precise interpretation of biogeochemical processes within sedimentary environments (Canfield and Thamdrup, 2009). Conventional redox-facies classifications, which focus on oxygen levels within the sediment, characterize environments arrayed along a complex biogeochemical gradient as ‘dysoxic’ or ‘anoxic’ (Canfield and Thamdrup, 2009). Similarly, geochemical facies classification schemes, including the Canfield-Thamdrup scheme, provide little insight into environmental gradients within ‘oxic’ environments. In oxic sedimentary environments, bioturbation indices reveal gradients in oxygen availability that controlled the distribution and size of benthic organisms (Drosser and Bottjer, 1986).

X-ray scanning data facilitate identification of Canfield-Thamdrup geochemical facies in the Hushpuckney Shale (Figure 8). Results derived from millimeter-scale core description and analysis of bulk abundance data for various sulfide-scavenged elements are consistent with those of previous workers (Algeo and Maynard, 2004; Algeo et al., 2004; Algeo and Heckel, 2008; Algeo and Maynard, 2008). The combination of XRF scanning and bioturbation indices facilitates our understanding of the benthic oxygen levels and provides a more comprehensive understanding of depositional environments in the North American mid-continent during the Pennsylvanian. The techniques

developed for this study can be used to identify the geochemical facies of shale deposits from other intervals.

The Hushpuckney Shale study core consists of a black shale submember overlain by a gray shale submember, indicating a general increase in benthic oxygen content during deposition, which was also noted by Algeo et al. (2004). The black shale submember exhibits laminations, absence of shelly and trace fossils, and high abundances of sulfide-scavenged elements, indicating deposition under conditions of severe oxygen depletion (Figure 8). In the overlying gray shale submember, the presence of trace fossils and relatively lower abundances of sulfide-scavenged elements indicate that oxygenated conditions prevailed during the deposition of these sediments (Figure 6).

The lowest layers of the black shale submember of the Hushpuckney Shale accumulated in an aerobic environment, as indicated by the presence of disrupted laminations and minute burrows (Bioturbation Index 2) in the shale immediately overlying the Middle Creek Limestone. Hence the oxygen level, though not high, was sufficient to allow a benthic community to develop. The remaining portion of the black shale submember accumulated in an oxygen-depleted environment. The ferruginous, sulfidic and the manganous-nitrogenous facies within the black shale are all assigned Bioturbation Index 1 based on the abundance of prominent, continuous apatite laminations and no evidence of bioturbation. The oxygen-depleted and quiet energy conditions prevalent during the deposition of the major portion of the black shale

submember provided perfect conditions for the formation of thick phosphatic bands, which exhibit the effects of winnowing and condensation.

The abundance of apatite nodules and laminae in the black shale submember of the study core suggest that this submember accumulated at a very slow rate under sediment-starved conditions (Heckel, 1977). Phosphatic laminae require several thousands of years to form in modern marine environments (Filippelli, 1997). Algeo et al. (2004) estimated that one centimeter of the black shale submember represented 500 to 2000 years of deposition. In their core, the black shale submember was 52 cm thick, and would have taken 26 to 104 kyr to accumulate.

In the study core, the maximum flooding surface (MFS) is placed at the top of the manganous-nitrogenous facies (~11366.60 - 11363.75 cm), between two prominent bands of apatite (Figure 1). XRF scanning data indicate abundance peaks of Ti and K between these bands (Figure 10). Minerals containing Ti and K have relatively high specific gravity and may become concentrated in deep ocean basins due to transportation and sorting by aeolian dust storms, or as a result of condensation (Jarvis et. al., 2001; Schaetzl and Loope, 2008). The presence of prominent apatite lamina in this region of the core suggests that a prolonged period of condensation, in a sediment-starved basin far away from the shore, may account for the abundance peaks of Ti and K associated with the MFS.

Oxygen content was lowest in the sulfidic facies, as evidenced by peaks observed in the abundance values of sulfide-scavenged elements, including Mo, Zn, V, Ni and Cr.

Sulfide-scavenged elements, including Mo, Zn, V, Ni and Cr, can distinguish sediments deposited under manganous-nitrogenous conditions from those deposited under sulfidic conditions (Brumsack, 2006; Tribovillard et. al., 2006: Table 1). Relative to the average marine shale, sulfide-scavenged trace elements are strongly enhanced under extreme conditions of oxygen-deficiency. In the present study, abundance peaks of Mo and Zn are used to indicate extremely sulfidic conditions (~ 11356 – 11360 cm: Figure 8). Although the geochemical profiles of Mo and Zn are similar, Mo exhibits stronger enrichment under sulfidic conditions than under ferruginous or manganous-nitrogenous conditions (Algeo and Lyons, 2006). If the hydrogen sulfide concentration exceeds a certain threshold limit (activity of free hydrogen sulfide ~ 11 μmol/l H_2S: Zheng et al., 2000), Mo is transformed into particle-reactive thiomolybdate, which is subsequently deposited as sediment (März et al., 2008). Widespread removal of Mo from the water column into the sediment occurs via metal sulfides and organic matter scavenging. Oxygen-deficient conditions, where hydrogen sulfide concentration falls below the threshold value, inhibit incorporation of Mo into sulfurized organic matter and pyrites (März et al., 2008). Alternatively, the rapid decline of Mo abundance values (Table 1) within the sulfidic facies can be attributed to the rapid depletion of Mo relative to other sulfide-scavenged elements within the water column. Zn exists as a free cation under oxygenated conditions, whereas in both weakly sulfidic and sulfidic conditions, Zn is removed from the water column in form of sulfides (Algeo and Maynard, 2004).

In the present study, sulfide-scavenged elements exhibit two different geochemical profiles (Figure 8). Mo and Zn exhibit peak abundance in the sulfidic facies

(~ 11356 – 11360 cm) whereas, V and Ni exhibit peak abundance across a wider interval of the sulfidic facies (~ 11338 – 11358 cm). Although the abundance peak of Cr is not as sharp as for other sulfide-scavenged elements, Cr peaks over an even wider interval (~ 11327 – 11351 cm). According to März et al. (2008), V has a mechanism of enrichment similar to Mo and Zn, but the abundance peak for V declines more slowly (Table 1). The gradual decline in the abundance of V may be due to its incorporation into other sedimentary fractions (organometallic ligands and geoporphyrins: März et al., 2008). In addition, higher concentrations of V in sea water relative to Mo and Zn may result in slower removal of V from the water column (März et al., 2008). März et al. (2008) did not consider Ni; however, in the Hushpuckney shale core, Ni exhibits a profile similar to V. Hence, it seems likely that V and Ni have similar enrichment mechanisms. Under oxygen-depleted conditions, Cr occurs in its reduced oxidation state, Cr(III), forming hydroxyl cations which become adsorbed to Fe- and Mn-oxyhydroxides, or form complexes with organic acids (Algeo and Maynard, 2004). Cr does not readily form sulfides and may even be lost to the water column by diffusion or advection during sediment transport. Moreover, Cr may be transported with the terrestrial clastic fraction into depositional basins (Tribovillard et. al., 2006). The complexity of Cr transport and enrichment in marine systems may account for the gradual decline in Cr abundance relative to that of Mo, Zn, V and Ni, thereby reducing its paleoenvironmental significance.

Although apatite nodules and lamina are abundant in the sulfidic facies, P/Ca ratios increase in the overlying manganous-nitrogenous facies (Figure 9). This increase

suggests that intense phosphorous precipitation took place as conditions in the water column changed from sulfidic to manganous-nitrogenous. During times of sulfidic bottom waters, phosphate was scavenged from organic matter and rapid formation of Fe-sulfides hindered the process of removal of phosphate by adsorbing in iron oxides, thereby delivering phosphate back to the water column (März et al., 2008). Hence, when conditions were favorable for deposition of sulfide-rich sediments, the concentration of dissolved phosphate within the oceanic waters increased significantly. After conditions changed from sulfidic to manganous-nitrogenous, syngenetic Fe-oxide precipitation at the chemocline resulted in phosphate removal in the water column and the subsequent deposition of apatite at the sea floor (März et al., 2008). Syngenetic iron minerals have large surface to volume ratios and high reactivity (Poulton and Canfield, 2006; Slomp et al., 1996). Because of this, these minerals are effective in scavenging phosphate from the water column. Thus during the deposition of the manganous-nitrogenous facies, dissolved phosphate in the water column was precipitated, resulting in higher P/Ca ratios within the sediment.

The gray shale submember was deposited under aerobic conditions favorable for a low diversity (worm dominated) benthic community (Algeo et al., 2004). At the aerobic burrowed facies overlying the contact between the gray shale and black shale submembers, there is a fossil lag, which indicates increased energy in the depositional environment. The remaining part of the gray shale submember consists of alternating layers aerobic homogenized sediment and aerobic burrowed sediment, indicating shifting oxygen content in the benthic waters. However, each individual facies within the

gray shale exhibits a range of bioturbation indices which indicates fluctuating biogeochemical conditions. In general, the stratigraphic increase in the benthic oxygen content during the deposition of the Hushpuckney shale including the black and the gray shale submembers, corresponds to the general decrease in the sea-level.

6. CONCLUSION

The method of classifying geochemical facies proposed by Canfield and Thamdrup (2009) can be used to evaluate depositional environments of the Hushpuckney Shale (Swope Formation, Kasimovian, Pennsylvanian). XRF scanning data coupled with X-radiography and bioturbation analysis enabled identification of sulfidic, ferruginous, manganous-nitrogenous, aerobic burrowed and aerobic homogenized facies.

The black shale submember of the Hushpuckney Shale has a high abundance of sulfide-scavenged trace elements. The base of the black shale submember has minute burrows and disrupted laminae, indicating that it accumulated in an oxygenated environment. The remainder of the black shale submember accumulated in an oxygen-depleted environment and consists of manganous-nitrogenous, ferruginous and sulfidic facies. The geochemical profiles of different sulfide-scavenged elements, including Mo, Zn, V, Ni, and Cr, contribute to our understanding of the biogeochemical processes of oxygen-depleted bottom water. During the deposition of the sulfidic facies, Mo, Zn, V, Ni and Cr were removed from the water column mainly in form of sulfides and deposited in the sediment. Among the sulfide-scavenged elements, Mo and Zn were readily precipitated under sulfidic conditions, but V, Ni and Cr exhibited delayed enrichment and gradual decline. This dissimilarity in the geochemical profiles of sulfide-scavenged elements can be attributed to faster drawdown of Mo and Zn, or to higher

concentration of V, Ni and Cr in the water column. Sulfidic conditions inhibited the removal of phosphate, resulting in the build-up of a large pool of dissolved phosphate in the basin. Subsequently, conditions changed and the oxygen-depleted bottom waters became non-sulfidic resulting in the deposition of the manganous-nitrogenous facies. At this time, dissolved phosphate sequestered in the water column was adsorbed onto, or precipitated with iron oxide minerals, thereby coupling Fe and P.

The gray shale submember has abundant trace fossils indicating deposition under oxic conditions. In combination with XRF scanning data, bioturbation indices are effective in classifying sediments of the gray shale submember into aerobic burrowed and aerobic homogenized facies.

REFERENCES

Algeo, T.J., Heckel, P.H., 2008. The Late Pennsylvanian Midcontinent Sea of North America: A review. Palaeogeogr. Palaeoclimatol. Palaeoecol. 268, 205–221.

Algeo, T.J., Lyons, T.W., 2006. Mo-total organic carbon covariation in modern anoxic marine environments: Implications for analysis of paleoredox and paleohydrographic conditions. Paleoceanography 21, PA1016, 1-23, doi: 10.1029/2004PA001112.

Algeo, T.J.,Maynard, J.B., 1997. Cyclic Sedimentation of Appalachian Devonian and Midcontinent Pennsylvanian Black Shales: Analysis of Ancient Marine Systems - A Combined Core and Field Workshop: Joint Meeting of Eastern Section: AAPG and The Society for organic Petrography (TSOP), Lexington, Kentucky, Sept 27-28. Department of Geology, University of Cincinnati, Cincinnati, pp. 147.

Algeo, T.J., Maynard, J.B., 2004. Trace element behavior and redox facies in core shales of Upper Pennsylvanian Kansas-type cyclothems. Chem. Geol. 206, 289-318.

Algeo, T.J., Maynard, J.B., 2008. Trace metal covariation as a guide to water-mass conditions in ancient anoxic marine environments. Geosphere 4, 872–887.

Algeo, T.J., Schwark, L., Hower, J.C., 2004. High-resolution geochemistry and sequence stratigraphy of the Hushpuckney Shale (Swope Formation, eastern Kansas): Implications for climate-environmental dynamics of the Late Pennsylvanian Midcontinent Seaway. Chem. Geol. 206, 259-288.

Arthur, M.A., Sageman, B.B., 1994. Marine Black Shales: Depositional mechanisms and environments of ancient deposits. Annu. Rev. Earth Planet. Sci. 22, 499-551.

Ayres, C.E., Jha, B.S., Meredith, H., Bowman, J.R., Bowlin, G.L., Henderson, S.C., Simpson, D.G., 2008. Measuring fiber alignment in electrospun scaffolds: A user's guide to the 2D fast Fourier transform approach. J. Biomater. Sci. Polymer Ed. 19, 603-621.

Brumsack, H.-J., 2006. The trace metal content of recent organic carbon-rich sediments: Implications for Cretaceous black shale formation. Paleogeog. Paleoclimatol. Paleoecol. 232, 344 - 361.

Canfield, D.E., Raiswell, R., Bottrell, S., 1992. The reactivity of sedimentary iron minerals toward sulfide. Amer. Journ. Sci. 292, 659–683.

Canfield, D. E., Thamdrup, B., 2009. Towards a consistent classification scheme for geochemical environments, or, why we wish the term 'suboxic' would go away. Geobiology 7, 385–392, doi: 10.1111/j.1472-4669.2009.00214.

Canfield, D.E., Thamdrup, B., Hansen, J.W., 1993. The anaerobic degradation of organic matter in Danish coastal sediments: Fe reduction, Mn reduction and sulfate reduction. Geochim. Cosmochim. Acta. 57, 3867–3883.

Codispoti, L.A., Brandes, J.A., Christensen, J.P., Devol, A.H., Naqvi, S.W.A., Paerl, H.W., Yoshinary, T., 2001. The oceanic fixed nitrogen and nitrous oxide budgets: Moving targets as we enter the anthropocene? Scientia Marina. 65, 85-105.

Croudace, I.W., Rindby, A., Rothwell, R.G., 2006. ITRAX: Description and evaluation of a new multi-function X-ray core scanner. In: Rothwell, R.G. (Ed.), New Techniques in Sediment Core Analysis. Geol. Soc. London. Spec. Publ., vol. 267, 51–63.

Cruse, A.M., Lyons, T.W., 2004. Trace metal records of regional paleoenvironmental variability in Pennsylvanian (Upper Carboniferous) black shales. Chem. Geol. 206, 319–345.

Droser, M.L., Bottjer, D.J., 1986. A semiquantitative classification of ichnofabric. J. Sed. Petrol. 56, 558-569.

Droser, M.L., Bottjer, D.J., 1988. Trends in depth and extent of bioturbation in Cambrian carbonate marine environments, Western United States. Geology 16, 223–236.

Filippelli, G.M., 1997. Controls on phosphorous concentration and accumulation in oceanic sediments. Mar. Geol. 139, 231-240.

Fitton, G., 1997. X-Ray fluorescence spectrometry. in: Gill, R. (Ed.), Modern Analytical Geochemistry: An Introduction to Quantitative Chemical Analysis for Earth, Environmental and Material Scientists. Addison Wesley Longman, Harlow, England. pp. 87-115.

Hebbeln, D., Cortés, J., 2001. Sedimentation in a tropical fjord: Golfo Dulce, Costa Rica. Geo-mar. Lett. 20, 142–148.

Heckel, P.H., 1977. Origin of phosphatic black shale facies in Pennsylvanian cyclothems of mid-continent North America. AAPG Bull. 61, 1045-1068.

Heckel, P.H., 1994. Evaluation of evidence for glacial-eustatic control over marine Pennsylvanian cyclothems in North America and consideration of possible tectonic effects. In: Dennison, J.M., Ettensohn, F.R. (Eds.), Tectonic and Eustatic Controls on Sedimentary Cycles. SEPM Concepts in Sedimentology and Paleontology 4, 65-87.

Jahn, B., Donner, B., Muller, P.J., Rohl, U., Schneider, R.R., Wefer, G., 2003. Pleistocene variations in dust input and marine productivity in the northern Benguela current: Evidence of evolution of global glacial-interglacial cycles. Palaeogeogr. Palaeoclimatol. Palaeoecol. 193, 515–533.

Jansen, J.H.F., Van der Gaast, S.J., Koster, B., Vaars, A.J., 1998. CORTEX, a shipboard XRF-scanner for element analyses in split sediment cores. Mar. Geol. 151, 143-153.

Jarvis, I., Murphy, A.M., Gale, A., 2001. Geochemistry of pelagic and hemipelagic carbonates: Criteria for identifying systems tracts and sea-level change. J. Geol. Soc. London 158, 685 – 696.

Kosanke, R.M., Cecil, C.B., 1996. Late Pennsylvanian climate changes and palynomorph extinctions. Rev. Paleobot. Palynol. 90, 113–140.

Kuypers, M.M.M., Sliekers, A.O., Lavik, G., Schmid, M., Jorgensen, B.B.,Kuenen, J.G., Damste, J.S.S., Strous, M., Jetten, M.S.M., 2003. Anaerobic ammonium oxidation by anammox bacteria in the Black Sea. Nature 422, 608-611.

März, C., Poulton, S.W., Beckmann, B., Küster, K., Wagner, T., Kasten, S., 2008. Redox sensitivity of P cycling during marine black shale formation: Dynamics of sulfidic and anoxic, non-sulfidic bottom waters. Geochim. Cosmochim. Acta 72, 3703–3717.

Morrison, J.M., Codispoti, L.A., Smith, S.L., Wishner, K., Flagg, C., Gardner, W.D., Gaurin, S., Naqvi, S.W.A., Manghnani. V., Prosperie, L., Gundersen, J.S., 1999. The oxygen minimum zone in the Arabian Sea during 1995. Deep-Sea Res. Part II 46, 1903-1931.

O'Brien, N.R., 1987. The effects of bioturbation on the fabric of shale. J. Sed. Petrol. 57, 449-455.

Peppers, R.A., 1996. Palynological correlation of major Pennsylvanian (Middle and Upper Carboniferous) chronostratigraphic boundaries in the Illinois and other coal basins. GSA Bul. 188, 1-111.

Percy, D., Li, X.N., Taylor, G.T., Astor, Y., Scranton, M.I., 2008. Controls on iron, manganese and intermediate oxidation state sulfur compounds in the Cariaco Basin. Mar. Geochem. 111, 47-62.

Postma, D., Appelo, C.A.J., 2000. Reduction of Mn-oxides by ferrous iron in a flow system: Column experiment and reactive transport modeling. Geochim. Cosmochim. Acta 64, 1237-1247.

Poulton, S.W., Canfield, D.E., 2006. Co-diagenesis of iron and phosphorous in hydrothermal sediments from the southern East Pacific rise: Implications for the

evaluation of paleoseawater phosphate concentrations. Geochim. Cosmochim. Acta 70, 5883 – 5898.

Rothwell, R.G., Hoogakker, B., Thomson, J., Croudace, I.W., Frenz, M., 2006. Turbidite emplacement on the southern Balearic Abyssal Plain (western Mediterranean Sea) during Marine Isotope Stages 1–3: An application of ITRAX XRF scanning of sediment cores to lithostratigraphic analysis. In: Rothwell, R.G. (Ed.), New Techniques in Sediment Core Analysis. Geol. Soc. London Spec. Publ., vol. 267, pp. 79–98.

Schaetzl, R.J., Loope, W.L., 2008. Evidence for an eolian origin for the silt-enriched soil mantles on the glaciated uplands of eastern Upper Michigan, USA. Geomorphology 100, 285-295.

Schieber, J., 2003. Simple gifts and buried treasures - implications of finding bioturbation and erosion surfaces in black shales. Sediment. Rec. 1 (2), pp. 4-8.

Schippers, A., Neretin, L.N., Lavik, G., Leipe, T., Pollehne. F., 2005. Manganese (II) oxidation driven bilateral oxygen intrusions in the western Black Sea. Geochim. Cosmochim. Acta 69, 2241-2252.

Schultz, R.B., 2004. Geochemical relationships of Late Paleozoic carbon-rich shales of the Midcontinent, USA: A compendium of results advocating changeable geochemical conditions. Chem. Geol. 206, 347-372.

Slomp, C.P., Van der Gaast, S.J., Van Raaphorst, W., 1996. Phosphorous binding by poorly crystalline iron oxides in North Sea sediments. Mar. Chem. 52, 55 – 73.

Tribovillard, N., Algeo, T.J., Lyons, T., Riboulleau, A., 2006. Trace metals as paleoresox and paleoproductivity proxies: An update. Chem. Geol. 232, 12 – 32.

Wignall, P.B., 1994. Black Shales, Clarendon Press, Oxford, England. 127 pp.

Zheng, Y., Anderson, R.F., van Geen, A., Kuwabara, J.S., 2000. Authigenic molybdenum formation in marine sediments: A linkage to pore water sulfide in the Santa Barbara Basin. Geochim. Cosmochim. Acta 64, 4165-4178.

APPENDIX

Table 1. Average gray values of elements in ferruginous and sulfidic facies. The gray values, which indicate the relative abundance of the selected elements, are calculated after lowess regression analysis and used in order to differentiate ferruginous and sulfidic facies within the Hushpuckney Shale.

Element	Ferruginous facies	Sulfidic facies
Mo	0.08 – 0.16	> 0.16
Zn	0.30 – 0.40	> 0.40
V	0.06 – 0.11	> 0.11
Ni	0.06 – 0.10	> 0.10

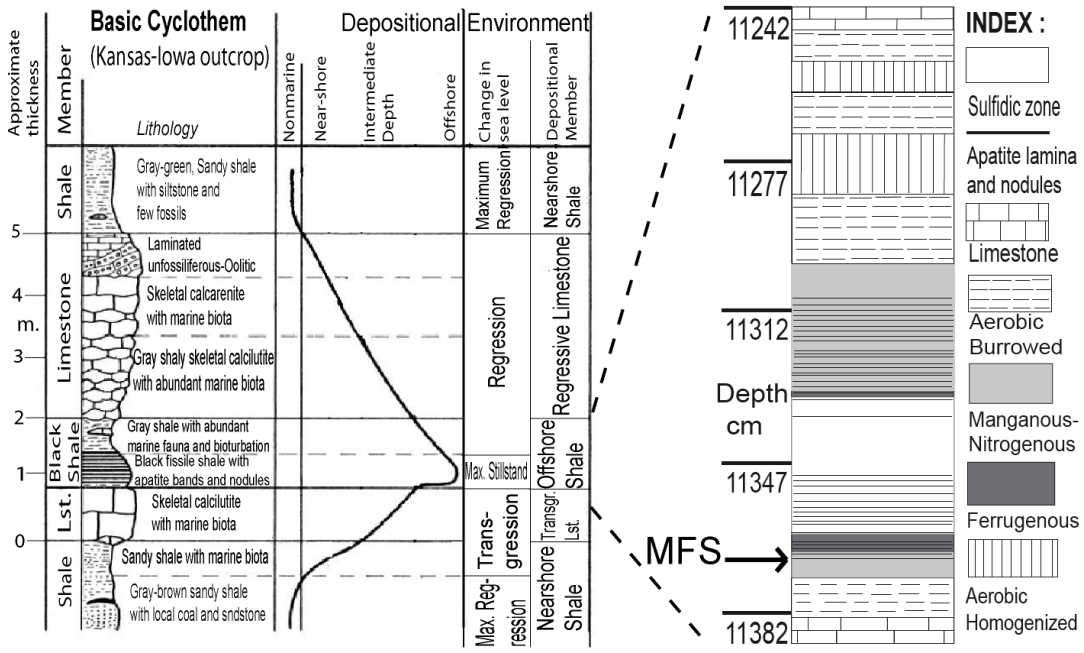

Figure 1. Cyclostratigraphy of Kansas-type cyclothemic core shales and inferred distribution of time. The stratigraphy of Hushpuckney shale and the correlative sea level curve is shown at the right hand side. (Algeo & Heckel, 2008). 'WBD' stands for Wind-blown dust interval.

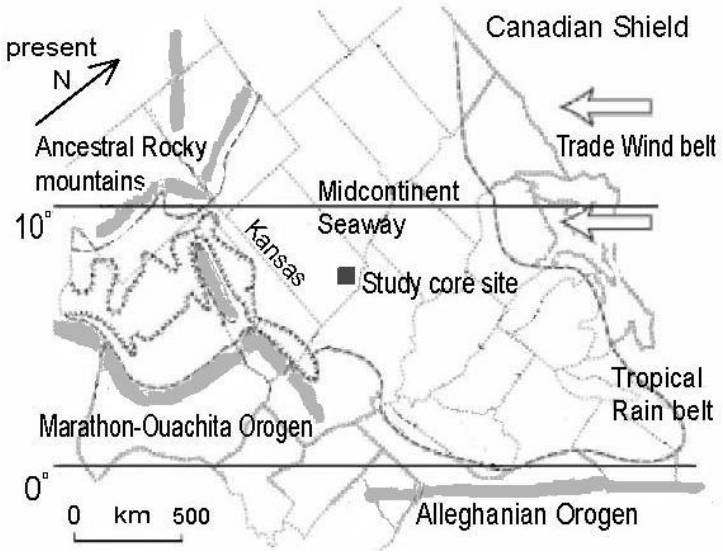

Figure 2. Paleogeography of Late Pennsylvanian North America (modified after Algeo et al., 2004 and Heckel, 1977). Dashed line indicates probable extent of the epicontinental seaway. Shaded gray areas represent different orogenic belts. At maximum transgression, the study site was located in the deeper parts of the Midcontinent Seaway far away from the shelf margins and paleoshorelines.

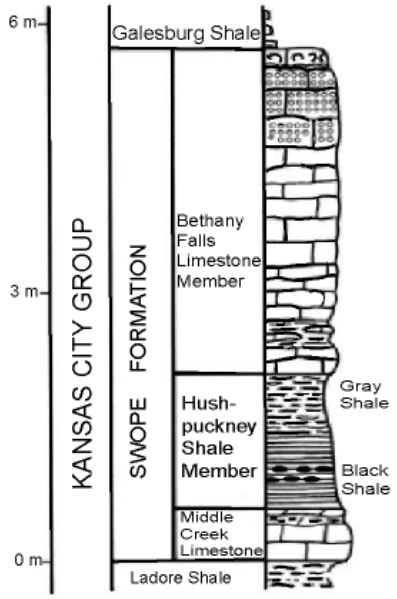

Figure 3. Generalized stratigraphic column of Kansas City Group in the outcrop.

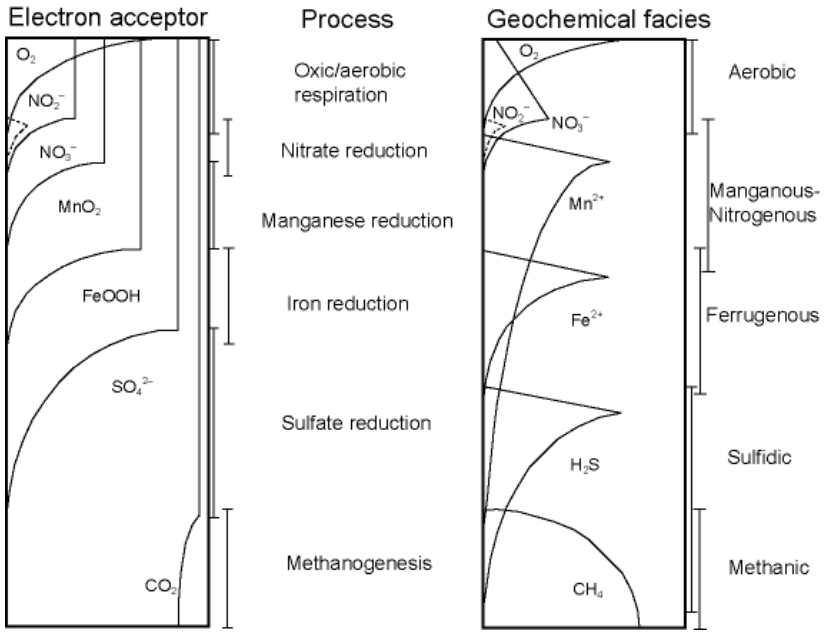

Figure 4. Depth distribution of common electron acceptors and the corresponding geochemical facies (modified after Caufield and Thamdrup, 2009)

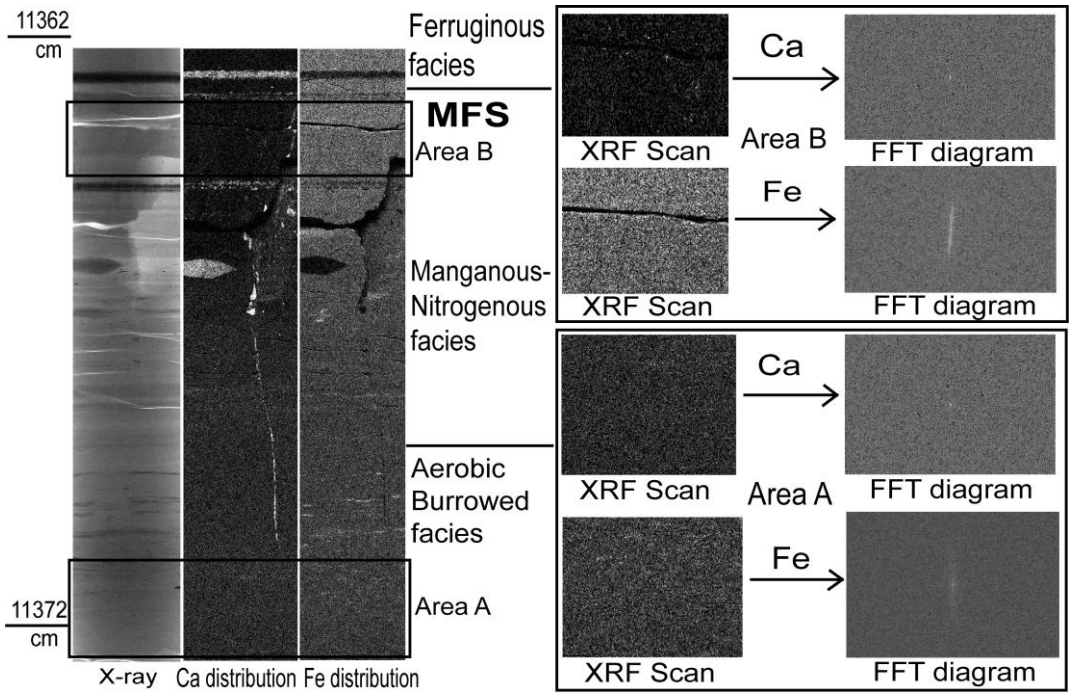

Figure 5. Iron laminations within the study core unit identified using the FFT technique.

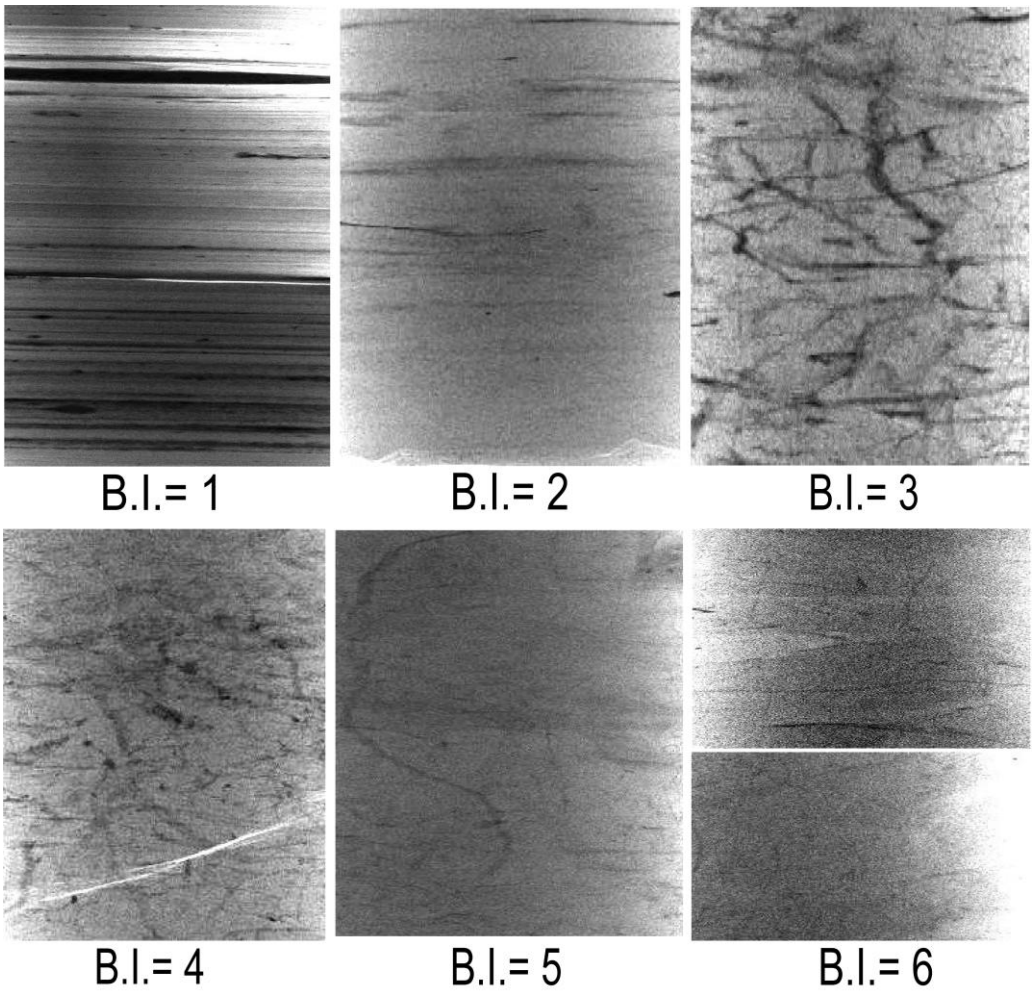

Figure 6. Bioturbation indices for the different geochemical facies of the Hushpuckney Shale.

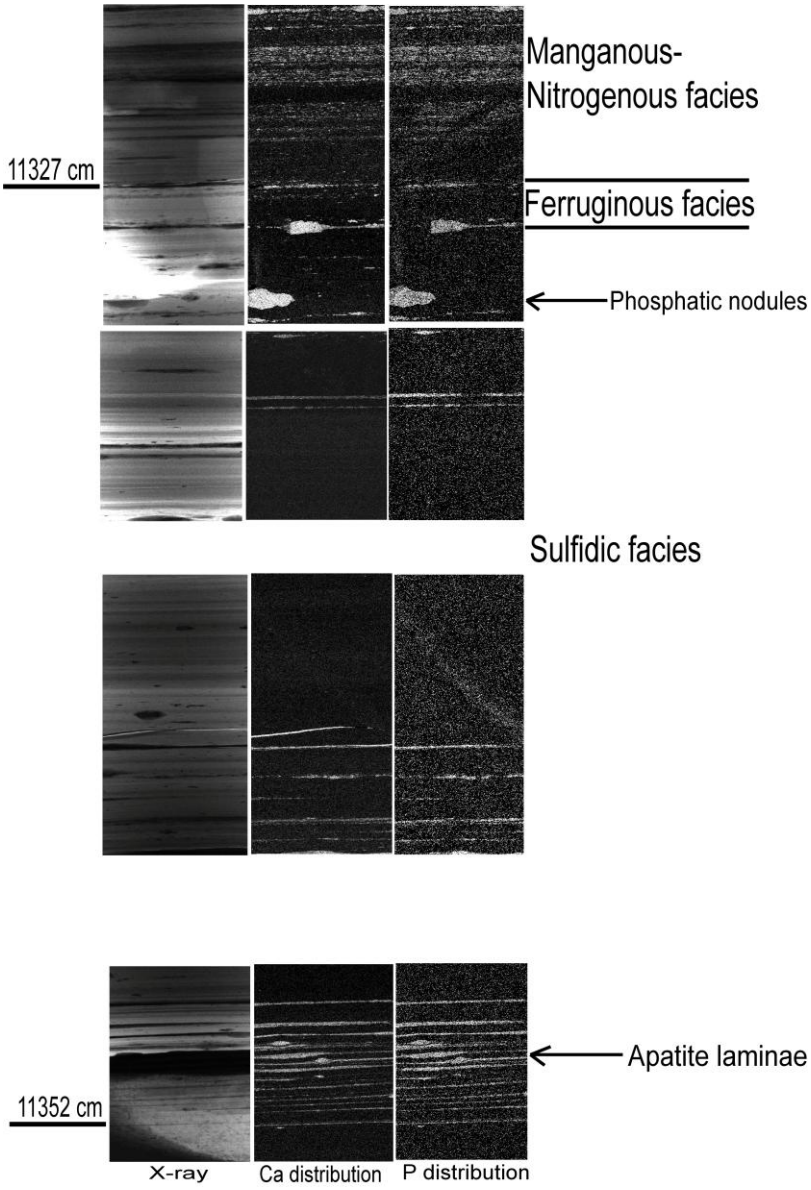

Figure 7. Laminations shown by apatite (Ca_3PO_4) within the study core. Abundant apatite nodules and bands are spread throughout the black shale submember.

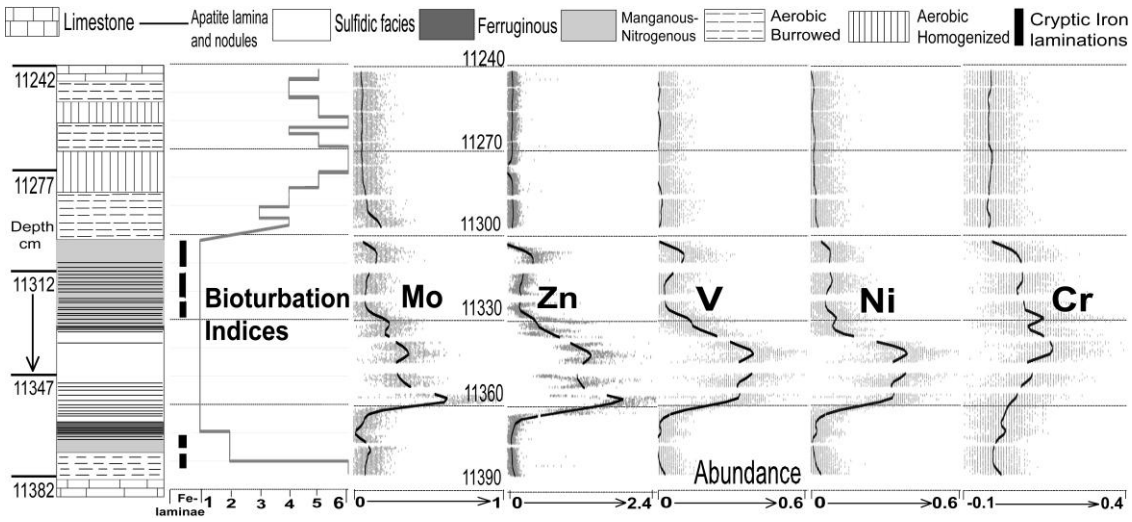

Figure 8. Relative abundance of various sulfide-scavenged elements (Mo, Zn, V, Ni, Cr) in the study core. Light gray dots represent the gray scale values and the dark line represents abundance values after lowess regression analysis. Gray bands in the last diagram indicate presence of cryptic iron laminations while thin, dark lines represent the bioturbation indices starting from 1 to 6.

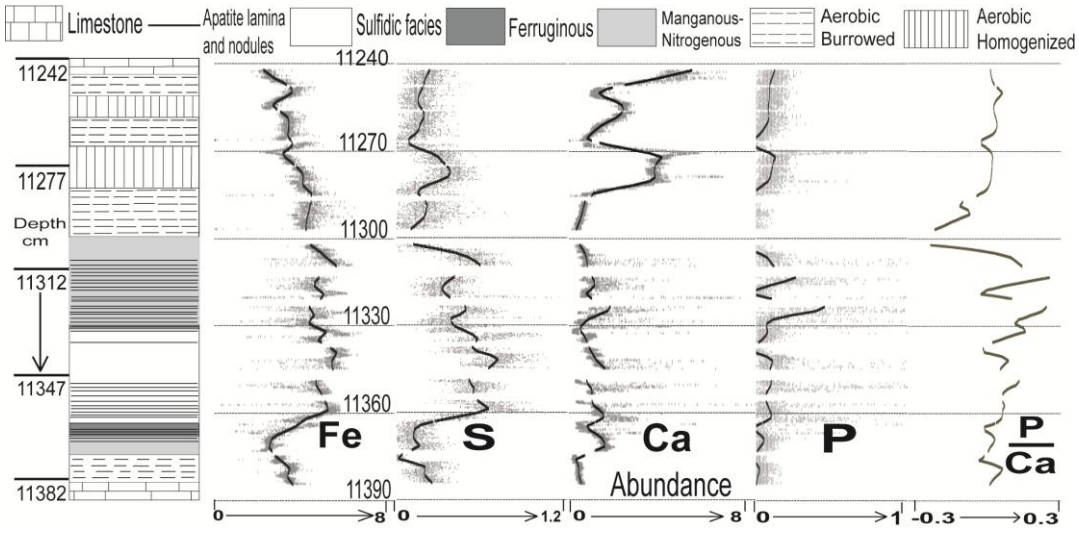

Figure 9. Relative abundance of various major elements (Fe, S, Ca, P) in the study core. P/Ca ratio indicates the presence of apatite especially within the black shale submember. Light gray dots represent the gray scale values and the dark line represents abundance values after lowess regression analysis.

VITA

Name: Sikhar Banerjee

Address: Mailstop# 3115, Department of Geology & Geophysics
Texas A&M University,
College Station, TX 77843

Email Address: sikhar.b@neo.tamu.edu

Education: B.S., University of Pune, 2006

M.S., Applied Geology, Indian Institute of Technology-Bombay, 2008

M.S., Geology, Texas A&M University, 2011